UAV Attitude Prediction using a new EKF and Stochastic Disturbed Process Noise Model

Belkacem Kada[*1], **Khalid Munawar**[#2], **Muhammad Shafique Shaikh**[#3], **Muhammad Bilal** [#4], **UbaidMuhsen Al-Saggaf** [#5]

[1]Aerospace Engineering Department, King Abdelaziz University,

[1,2,3,4,5]Department of Electrical Engineering and Computer Science, King Abdelaziz University,

Corresponding author: [1]bkada@kau.edu.sa

[2]kmunawar@kau.edu.sa, [3]shafique2ms@gmail.com, [4]msmuhammad@kau.edu.sa, [5]usaggaf@kau.edu.sa

Abstract

Even though low-cost inertial navigation units (INS) are affordable, their data gathering is often of low quality and accuracy. In addition, the nonlinear nature of process and measurement models renders those INS incapable of delivering accurate navigation for airborne vehicles. Given the constraint that MEMS sensors used in low-cost INS design offer signals with bias variations and large amounts of noise, the present paper aims to design an EKF for low-cost UAV attitude estimation using a perturbed process noise model and a nonlinear measurement estimator. The UAV orientations are obtained using a data fusion model that uses accelerometers and magnetometer measurements gathered from field experiments. First-order Gauss-Markov models and zero-mean Gaussian noises are used to model biases and measurement noises, respectively. Simulation results reveal that the proposed method can effectively estimate the UAV attitude with high precision and cheap cost, both of which have practical applications in flight control systems.

1.   Introduction

Cost-effective Unmanned Aerial Vehicle (UAV) platforms are becoming increasingly popular in the civilian and military aviation sectors for various tasks, including surveillance, reconnaissance, and inspection. The Inertial Navigation Systems (INS) in these automobiles typically utilize low-cost and low-power inertial sensing technology developed for use in Micro-Electro-Mechanical Systems (MEMS). Unlike other types of gyroscopes, such as active ring-laser and interferometric fiber-optic sensors, MEMS gyros are less precise, noisier, more sensitive to external impacts, and have larger biases [1,2]. Also, MEMS-based INS can't directly estimate orientation in the air. If MEMS-based INS need to be reliable and accurate

enough for UAV attitude monitoring and estimation, Nonlinear filtering and data fusion are of prime importance.

On the other hand, Extended Kalman Filter (EKF) and Gauss-Markov models are popular filters and estimators used for attitude estimate, tracking, nonlinear measurement, bias, and uncertainty modeling [3-8]. However, in numerous attitude estimation applications, the linearization inherent to EKF results in performance deterioration and unbounded estimation errors. This is due mainly to highly nonlinear dynamics, nonlinear measurement models, and the absence of reasonable priori state estimates. Various nonlinear attitude estimation approaches with enhanced robustness and precision have been developed in response to these limitations. Optimal Kalman Filter (OKF), Particle Filters (PFs), and the Generalized Complementary Extended Kalman Filter (GCEKF) are among the valuable alternatives to the conventional EKF [9].

Recently, nonlinear filtering for flying vehicles' attitude estimation has received growing interest. The mission of autonomous vehicles such as UAVs requires high-precision attitude prediction. Among the most recent studies in UAV attitude estimation using nonlinear filters, one can cite the comparison study between EKF and UKF for attitude estimation of a fixed-wing UAV presented in [10], in which the authors demonstrated that UKF exhibits superior performance and robustness compared to EKF. In the presence of Gaussian process and measurement disturbances, the authors of [11] recommended utilizing OKF to estimate the state variables of a quadrotor UAV. Despite disturbances, accurate location and attitude monitoring were predicted using OKF. In the research presented in [12], Particle optimization Swarm (POS) was applied successfully for attitude estimation of a fixed-wing UAV in dynamic environments. In [13], the authors presented a novel GCEKF method based on vector observation. Using cross-products, this inventive method estimated and compensated for attitude errors. In [14], a complementary filter-based attitude estimation method was proposed in which the gyroscope's output angular velocity was obtained by combining the acceleration measured by an accelerometer and the magnetic field measured by a magnetometer. Using a cheap navigation device with an IMU, ultrasonic range sensors, and an optical flow camera, the authors in [15] designed a Kalman filtering-based sensor fusion system for navigation in areas where global positioning system (GPS) signals are blocked. To deal with heterogeneous sensors with varying sample rates, a multi-rate EKF was proposed. The results demonstrated high precision and stability of the attitude estimation technique. In [16], authors presented an EKF for a low-budget MARK sensor setup (magnetic, angular rate, and gravity). The proposed method combines the EKF with a two-stage gradient descent algorithm (GDEKF). The attitude angles were first adjusted using the accelerometer and magnetometer in a two-stage gradient descent technique. The gyroscope's computed attitude and bias were adjusted using quaternions in conjunction with the gyroscope measurement values. The outcomes demonstrated the proposed filter's effectiveness in measurement accuracy, anti-interference performance, and dynamic performance. However, most of the previously mentioned filters are uncertain or unstable due to UAVs' rapid attitude dynamics and substantial measurement error systems [17-20].

Nonlinear filtering methodologies for UAV attitude estimation depend on its kinematics representation and observation modeling. Conventional EKF-based estimators are either singular or redundant [21]. Further, in low-cost UAV technologies, the IMU system comprises low-performance gyros, accelerometers, and magnetometers, making them susceptible to errors and noises, including bias and measurement-corrupted noises. Significant guidance, navigation, and control issues arise when biases are integrated into the mechanization process. To overcome this dilemma, a new perturbed process noise-based EKF design for a low-cost UAV attitude estimation is proposed in the present study. To demonstrate the effectiveness of the proposed filter, the attitude, and gyros measurement biases of the UltraStick e25 UAV are estimated using flight test data. White Gaussian noises are used to introduce process and measurement noises, and first-order Gauss-Markov processes are used to model the gyro biases.

2. Extended Kalman Filter And Sensitivity Analysis

2.1 Extended Kalman filter design

Consider the following nonlinear dynamic system

$$\begin{cases} \dot{x}(k) = f(x(k-1), u(k), w(k)) \\ y(k) = h(x(k), v(k)) \end{cases} \qquad (1)$$

where $f \in \mathbb{R}^n$ and e $h \in \mathbb{R}^m$ are differential field vectors; $x \in \mathbb{R}^n, u \in \mathbb{R}^p$, $y \in \mathbb{R}^m$ denote the system state vector, the control vector, and the output vector, respectively; $w \in \mathbb{R}^n$, $v \in \mathbb{R}^m$ are the process noise and the sensor-noise input, respectively. It is a common practice to implement nonlinear Kalman filters using state-space-based algorithms that combine model and measurement data to produce an optimal state estimation.

Stage 1: Time update

As shown in the following equation, the filter first generates a current estimate (prediction) of the system state vector x and its associated error covariance matrix P for time $'k'$ based on the previous estimate and error covariance matrix at time $'k'$

$$\begin{cases} x(k|k-1) = f(x(k-1|k-1), u(k), w(k)) \\ P(k|k-1) = \mathbf{F}(k|k-1)P(k-1|k-1)\mathbf{F}^T(k|k-1) + L(k)Q(k)L^T(k) \\ y(k) = h(x(k|k-1), v(k)) \end{cases} \qquad (2)$$

Table 1. EKF predict variables

Variable	Definition
k	Time step
$x(k|k-1)$	Prior estimate
$P(k|k-1)$	Prior estimation-error covariance

$F(k\|k-1)$	State transition model
$L(k)$	Process noise model
$Q(k)$	Process noise covariance

where $F = \partial f/\partial x \in \mathbb{R}^{n \times n}$, $L = \partial f/\partial w \in \mathbb{R}^{n \times n}$ and $h(.)$ is an observation nonlinear vector function. The following condition, which rules out any overconfidence in the estimate $\hat{x}$, must be verified by the matrix P in order to ensure internal consistency

$$P(k|k-1) - cov[x(k|k-1) - \hat{x}(k|k-1)] \geq 0 \qquad (3)$$

Stage 2: Measurement update

Using an observation model, the a priori estimate derived in stage 1 (Eq. 10) is adjusted. Compared to the prior estimates, the following posteriori state and error covariance matrices have a smaller standard error

$$\begin{cases} x(k|k) &= x(k|k-1) + K(k)e(k) \\ P(k|k) &= \big(I - K(k)H(k)\big)P(k|k-1) \end{cases} \qquad (4)$$

with $e(k)$ and $K(k)$ being the innovation and Kalam gain matrix, respectively

$$\begin{cases} e(k) = [y(k) - H(k)x(k|k-1)] \\ K(k) = P(k|k-1)H^T(k)S^{-1}(k) \\ S(k) = [H(k)P(k|k-1)H^T(k) + M(k)R(k)M^T(k)] \end{cases} \qquad (5)$$

where $H(k) = \partial h(x(k|k-1))/\partial x(k|k-1) \in \mathbb{R}^{p \times n}$ denotes the observation model matrix $M = \partial h(x(k|k-1))/\partial v(k|k-1) \in \mathbb{R}^{n \times p}$ denote and the measurement noise model matrix, respectively. It is worth noting that F, L, and H are Jacobian matrices and $y(k) - H(k)x(k|k-1)$ represents the discrepancy between actual measurements $y(k)$ and predicted ones $H(k)x(k|k-1)$.

Table 2. EKF update variables

Variable	Definition
$x(k\|k)$	Posterior estimate
$P(k\|k)$	Posterior estimation-error covariance
$F(k\|k-1)$	State transition model
$e(k)$	Innovation
$K(k)$	Filter gain matrix
$S(k)$	Estimator gain matrix
$H(k)$	Measurement matrix

$R(k)$	Measurement noise covariance

2.2 Sensitivity analysis

Consider the case $u(k) = 0$, the EKF (2)- (5) is written as follows

$$\begin{cases} x(k|k-1) = \mathbf{F}(k)x(k-1) + L(k)w(k) \\ P(k|k-1) = \mathbf{F}(k)P(k-1|k-1)\mathbf{F}^T(k) + L(k)Q(k)L^T(k) \\ y(k) = H(x(k|k-1), v(k)) \\ x(k|k) = x(k|k-1) + K(k)[y(k) - H(k)x(k|k-1)] \\ P(k|k) = (I - K(k)H(k))P(k|k-1) \\ K(k) = P(k|k-1)H^T(k)[H(k)P(k|k-1)H^T + M(k)R(k)M^T(k)]^{-1} \end{cases} \quad (6)$$

To start sensitivity analysis of the EKF (6), we make the following assumptions

Assumption 1. $L = M = I$.

Assumption 2. Q and R are symmetric.

Assumption 3. There exists an orthogonal matrix Λ such that $\Lambda^T Q \Lambda$, $\Lambda^T R \Lambda$, $\Lambda^T P(k-1|k-1)\Lambda$ and $\Lambda^T P(k|k)\Lambda$ are diagonal matrices.

Assumption 4. $Q = Q_t + \delta Q$ where Q_t and δQ denote the covariance of the true process noise and a fictitious process noise, respectively.

For simplicity, we drop the notation 'k' from all the matrices expect for P and we substitute $P(k|k)$ witn $P_{k,k}$. From equation (6), using assumption 1, $P_{k,k}$ can be written as follows

$$\begin{aligned} P_{k,k} &= (I - KH)P_{k,k-1} \\ &= (I - P_{k,k-1}H^T[HP_{k,k-1}H^T + R]^{-1}H)P_{k,k-1} \\ &= (I - [\mathbf{F}P_{k-1,k-1}\mathbf{F}^T + Q]H^T[H(\mathbf{F}P_{k-1,k-1}\mathbf{F}^T + Q)H^T + R]^{-1}H) \cdot [\mathbf{F}P_{k-1,k-1}\mathbf{F}^T + Q] \end{aligned}$$
$$(7)$$

Consider the case $H = I$

$$P_{k,k} = (I - [\mathbf{F}P_{k-1,k-1}\mathbf{F}^T + Q][(\mathbf{F}P_{k-1,k-1}\mathbf{F}^T + Q) + R]^{-1}) \cdot [\mathbf{F}P_{k-1,k-1}\mathbf{F}^T + Q]$$
$$(8)$$

Using assumption 3,

$$\begin{aligned} P_{k,k} = \Lambda(I - [\Lambda\mathbf{F}P_{k-1,k-1}\mathbf{F}^T\Lambda^T + \Lambda Q\Lambda^T][(\Lambda\mathbf{F}P_{k-1,k-1}\mathbf{F}^T\Lambda^T + \Lambda Q\Lambda^T) + \Lambda R\Lambda^T]^{-1}) \cdot \\ [\Lambda\mathbf{F}P_{k-1,k-1}\mathbf{F}^T\Lambda^T + \Lambda Q\Lambda^T]\Lambda^T \end{aligned}$$
$$(9)$$

Assume $\Lambda R\Lambda^T = \Omega$,

$$\begin{aligned} \Lambda P_{k,k}\Lambda^T = (I - [\Lambda\mathbf{F}P_{k-1,k-1}\mathbf{F}^T\Lambda^T + \Lambda Q\Lambda^T][\Lambda\mathbf{F}P_{k-1,k-1}\mathbf{F}^T\Lambda^T + \Lambda Q\Lambda^T + \Omega]^{-1}) \cdot \\ [\Lambda\mathbf{F}P_{k-1,k-1}\mathbf{F}^T\Lambda^T + \Lambda Q\Lambda^T] \end{aligned}$$
$$(10)$$

Since $\boldsymbol{\Lambda P}_{k,k}\boldsymbol{\Lambda}^T$ is diagonal, it results from equation (10) and assumption (4) that the eigenvalue $\tilde{P}_{i,k}$ is given as follows

$$\tilde{P}_{i,k} = \left(\left(\tilde{f}_{i,k-1}^2 \tilde{P}_{i,k-1} + \tilde{q}_i + \delta\tilde{q}_i \right) - \frac{\left(\tilde{f}_{i,k-1}^2 \tilde{P}_{i,k-1} + \tilde{q}_i + \delta\tilde{q}_i \right)^2}{\tilde{f}_{i,k-1}^2 \tilde{P}_{i,k-1} + \tilde{q}_i + \delta\tilde{q}_i + \lambda_i} \right) \tag{11}$$

where $\tilde{P}_{i,k-1}$, $\tilde{f}_{i,k-1}$, $\tilde{q}_i$, $\delta\tilde{q}_i$, and λ_i denote the eigenvalues of $\boldsymbol{P}_{k-1,k-1}$ $\mathbf{F}$, $\boldsymbol{Q}_t$, $\delta\boldsymbol{Q}$ and $\boldsymbol{\Omega}$, respectively. Equation (11) shows that the eigenvalues $\tilde{P}_{i,k}$ depend on the process noise covariance eigenvalues $\tilde{q}_i$ and the measurement noise covariance eigenvalues λ_i. First, the gradient of $\tilde{P}_{i,k}$ with respect to the eigenvalue $\delta\tilde{q}_i$ is given, from equation (11), as follows

$$\Delta\tilde{P}_{i,k} = \frac{\partial\tilde{P}_{i,k}}{\partial\delta\tilde{q}_i}\bigg|_{\delta\tilde{q}_i=0} \delta\tilde{q}_i = \left(1 - \frac{2\left(\tilde{f}_{i,k-1}^2 \tilde{P}_{i,k-1} + \tilde{q}_i + \delta\tilde{q}_i\right)\left(\tilde{f}_{i,k-1}^2 \tilde{P}_{i,k-1} + \tilde{q}_i + \delta\tilde{q}_i + \lambda_i\right) - \left(\tilde{f}_{i,k-1}^2 \tilde{P}_{i,k-1} + \tilde{q}_i + \delta\tilde{q}_i\right)^2}{\left(\tilde{f}_{i,k-1}^2 \tilde{P}_{i,k-1} + \tilde{q}_i + \delta\tilde{q}_i + \lambda_i\right)^2} \right) \delta\tilde{q}_i$$

$$= \left(1 - \frac{2\left(\tilde{f}_{i,k-1}^2 \tilde{P}_{i,k-1} + \tilde{q}_i + \delta\tilde{q}_i + \lambda_i\right) - \left(\tilde{f}_{i,k-1}^2 \tilde{P}_{i,k-1} + \tilde{q}_i + \delta\tilde{q}_i\right)}{\left(\tilde{f}_{i,k-1}^2 \tilde{P}_{i,k-1} + \tilde{q}_i + \delta\tilde{q}_i + \lambda_i\right)} \right) \delta\tilde{q}_i$$

$$= \left(1 - \frac{\left(\tilde{f}_{i,k-1}^2 \tilde{P}_{i,k-1} + \tilde{q}_i + \delta\tilde{q}_i + 2\lambda_i\right)}{\left(\tilde{f}_{i,k-1}^2 \tilde{P}_{i,k-1} + \tilde{q}_i + \delta\tilde{q}_i + \lambda_i\right)} \right) \delta\tilde{q}_i \tag{12}$$

Next, using equation (12), the sensitivity $\Delta\tilde{P}_{i,k}$ with respect to λ_i can be addressed as follows

$$\frac{\partial\Delta\tilde{P}_{i,k}}{\partial\lambda_i} = -\frac{2\left(\tilde{f}_{i,k-1}^2 \tilde{P}_{i,k-1} + \tilde{q}_i + \delta\tilde{q}_i + \lambda_i\right) - \left(\tilde{f}_{i,k-1}^2 \tilde{P}_{i,k-1} + \tilde{q}_i + \delta\tilde{q}_i + 2\lambda_i\right)}{\left(\tilde{f}_{i,k-1}^2 \tilde{P}_{i,k-1} + \tilde{q}_i + \delta\tilde{q}_i + \lambda_i\right)^2} \delta\tilde{q}_i$$

$$= -\frac{\left(\tilde{f}_{i,k-1}^2 \tilde{P}_{i,k-1} + \tilde{q}_i + \delta\tilde{q}_i\right)}{\left(\tilde{f}_{i,k-1}^2 \tilde{P}_{i,k-1} + \tilde{q}_i + \delta\tilde{q}_i + \lambda_i\right)^2} \delta\tilde{q}_i \tag{13}$$

Since $\boldsymbol{\Lambda R \Lambda}^T = \boldsymbol{\Omega}$ is a positive semidefinite matrix with $\lambda_i \geq 0$, we conclude that

$$\frac{\partial\Delta\tilde{P}_{i,k}}{\partial\lambda_i} < 0, \qquad for \ \ \delta\tilde{q}_i > 0 \tag{14}$$

From equation (12), one can find that

$$\begin{cases} \lim_{\lambda_i \to 0} \Delta\tilde{P}_{i,k} = 0 \\ \lim_{\lambda_i \to \infty} \Delta\tilde{P}_{i,k} = -\delta\tilde{q}_i \end{cases} \tag{15}$$

Equation (15) shows that $\lim_{\lambda_i \to 0} \Delta\tilde{P}_{i,k}(\lambda_i)$ decreases monotonically as $\lambda_i \to \infty$.

3.   Ekf-Based Uav Attitude Estimation

In this section, we applied the EKF shown in section 2 to a fixed-wing UAV attitude estimation to demonstrate its effectiveness and sensitivity.

3.1 UAV Attitude parametrization

The orientation of an aircraft, as described by Euler Angles (EA), is determined by three successive revolutions with respect to a fixed inertial reference, with the order of the rotations being of utmost importance. In a fixed reference frame, the relationships between angular velocities and EA are

$$\begin{cases} p = \dot{\phi} - \sin\theta\,\dot{\psi} \\ q = \cos\phi\,\dot{\theta} + \sin\phi\cos\theta\,\dot{\psi} \\ r = -\sin\phi\,\dot{\phi} + \cos\phi\cos\theta\,\dot{\psi} \end{cases} \qquad (16)$$

where ϕ, θ, ψ, p, q, and r denote the roll, pitch, and yaw rotation angles and their corresponding rates, respectively. Integrating the following equations, which are derived from a simple rearrangement of the original equations (16), gives the orientations of the airframe

$$\begin{cases} \dot{\phi} = p + (q\sin\phi + r\cos\phi)\tan\theta \\ \dot{\theta} = q\cos\phi - r\sin\phi \\ \dot{\psi} = (q\sin\phi + r\cos\phi)/\cos\theta \end{cases} \qquad (17)$$

In matrix form, we get

$$\begin{Bmatrix} \dot{\phi} \\ \dot{\theta} \\ \dot{\psi} \end{Bmatrix} = \begin{bmatrix} 1 & \sin\phi\tan\theta & \cos\phi\tan\theta \\ 0 & \cos\phi & -\sin\phi \\ 0 & \dfrac{\sin\phi}{\cos\theta} & \dfrac{\cos\phi}{\cos\theta} \end{bmatrix} \begin{Bmatrix} p \\ q \\ r \end{Bmatrix} \qquad (18)$$

Despite drawbacks in EA-based attitude prediction algorithms like drift error accumulation, the gimbal-lock problem, and a lack of robustness against disturbances, non-full range nonlinear filters can be efficiently developed based on EA for smooth flight trajectories. Parameter adaptability and non-cumulative error-adding systems, such as magnetometers, can enhance robustness and performance.

3.2 EKF for attitude estimation

In the basis of Euler angles, we propose an EKF to predict the attitude of an UAV airframe. In this study we define the state vector as $\boldsymbol{x} = \begin{bmatrix} \phi & \theta & \psi & b_p & b_q & b_r \end{bmatrix}^T$ and the vector $\boldsymbol{u} = \boldsymbol{\omega}^T = [p\ \ q\ \ r]^T$. The state and measurement equations in model (2) are given as follows

$$\begin{cases} \boldsymbol{x}_k = \boldsymbol{F}_{k,k-1}\boldsymbol{x}_k + \boldsymbol{G}_{k,k-1}\boldsymbol{u}_k + \boldsymbol{w}_k \\ \boldsymbol{y}_k = \boldsymbol{x}_m + \boldsymbol{v}_k \end{cases} \qquad (19)$$

with the matrices $\boldsymbol{F}$ and $\boldsymbol{G}$ are given by

$$\mathbf{F} = \begin{bmatrix} 0_{3\times3} & \boldsymbol{T} \\ 0_{3\times3} & 0_{3\times3} \end{bmatrix}, \qquad \boldsymbol{G} = \begin{bmatrix} \boldsymbol{T} \\ 0_{3\times3} \end{bmatrix} \qquad (20)$$

$$\boldsymbol{T} = \begin{bmatrix} 1 & \sin\phi\tan\theta & \cos\phi\tan\theta \\ 0 & \cos\phi & -\sin\phi \\ 0 & \sin\phi/\cos\theta & \cos\phi/\cos\theta \end{bmatrix} \qquad (21)$$

where $\boldsymbol{b} = \begin{bmatrix} b_p & b_q & b_r \end{bmatrix}^T$ denotes the gyros biases vector, b_p, b_q and b_r are the roll, pitch, and yaw gyros biases, respectively. The transformation matrix $\boldsymbol{T}$ converts body-frame angular rates to Euler angular rates. The output vector $\boldsymbol{y}_k$ in model (19) is supplied by the magnetometer and attitude biases. Magnetometers are effective Bayesian recursive filters for correcting errors induced by inertial measurements. Using magnetometer readings, the UAV's attitude is computed as follows

$$y = \begin{bmatrix} \phi_m & \theta_m & \psi_m & b_{p_m} & b_{q_m} & b_{r_m} \end{bmatrix}^T \quad (22)$$

$$\begin{cases} \phi_m = -a\,tan\,2\left(\dfrac{a_y}{\sqrt{a_y^2 + a_z^2}}\right) \\[2mm] \theta_m = -a\,sin\left(\dfrac{a_y}{g}\right) \\[2mm] \psi_m = -a\,tan\,2\left(\dfrac{h_y\cos\phi_m - h_z\sin\phi_m}{h_x\cos\theta_m + h_y\sin\phi_m\sin\theta_m + h_z\cos\phi_m\sin\theta_m}\right) \end{cases} \quad (23)$$

where h_x,h_y,h_z and a_x,a_y,a_z are the earth's magnetic field and linear accelerations measured along x, y and z aircraft body axes, respectively; g denotes the gravitational acceleration with gravity reference vector defined as follows

$$n = \begin{bmatrix} n_x & n_y & n_z \end{bmatrix}^T = \begin{bmatrix} 0 & 0 & -1 \end{bmatrix}^T \quad (24)$$

3.3 Nonlinear measurement, bias, and uncertainties modeling

Many factors, including nonlinear dynamics, unmodeled dynamics, modeling uncertainties, and measurement errors, can cause the EKF to diverge and produce biased estimates. To implement the EKF (2)-(5), it is assumed that the process and measurement noises are uncorrelated time-independent Gaussian white noises with $cov(w_k, v_k) = 0$ and $cov(w_k, x_0) = cov(v_k, x_0) = 0$

$$\begin{cases} E\{w_k\} = E\{v_k\} = 0 \\ E\{w_k w_l^T\} = Q\delta_{kl} \\ E\{v_k v_l^T\} = R\delta_{kl} \end{cases} \quad (25)$$

where δ_{kl} denotes the Kronecker delta. The following model updates the sensors measurements when non-static bias is present.

$$y_m = y + b + \Gamma\rho \quad (26)$$

where y and y_m denote the true value and the sensor value vectors, respectively. Γ is a full rank weighting matrix, and ρ denotes the measurement noise, considered, in this study as an independent Gaussian random variable

$$\begin{cases} E\{\rho_k\} = 0 \\ E\{\rho_k \rho_l^T\} = \sigma^2 I\delta_{kl} \end{cases} \quad (27)$$

In the measurement model (26), b represents a first-order Gauss-Markov process

$$\dot{b} = -\frac{1}{\gamma}b + z \quad (28)$$

where γ, z denote the correlation time (Gauss-Markov time constant) and Brownian noise process, respectively, and σ denotes the noise variance.

4.   Field Experiment And Simulation Study Results

The purpose of this section is to evaluate the accuracy of estimating the three attitude angles of an UAV frame as well as the convergence of the EKF. The flight test was performed using the fixed-wing UltraStick e25 airframe and handled manually with a typical radio control unit in an open-loop control. A complete takeoff-to-landing flight mission was performed with different maneuvers over 200 seconds. We acquired flight test data and transmitted telemetry, with typical sensor biases displayed in Table 3. It is worth noting that the UltraStick airframe has been successfully used as a low-cost test platform for model-aided navigation, guidance, and control system research at NASA Langley Research Center.

Table 3. Typical biases and random errors for sensors

Instrument	Bias Variance (all axes)	Random Error (all axes)
Gyros	$\pm 3 \ (deg/s)$	$\pm 1 \ (deg/s)$
Accelerometers	$\pm 0.05 \ (m/s^2)$	$\pm 0.009 (m/s^2)$
Magnetometer	$\pm 4 \ (mG)$	$\pm 1.25 \ (mG)$

A test flight was conducted at a cruising speed of 50 (m/s) to evaluate the proposed filter's sensitivity to high seed perturbation. (i.e., higher than the aircraft cruise speed). To account for the EKF's sensitivity to the errors and uncertainties mentioned above, the process and measurement covariances are chosen as follows

$$\begin{cases} Q = diag(\sigma_1^2, \dots, \sigma_6^2) + \delta q I_{6x6} \\ R = diag(\mu_1^2, \dots, \mu_6^2) \end{cases} \qquad (29)$$

where σ_i and μ_i denote the standard deviations of process noise and measurement noise, respectively. Since the numerical simulation requires discrete-time dynamic models, the matrix Q must be small (i.e., close to zero but not zero). We set $\sigma_i = 0.01$ and $\delta q = 0.1$, and μ_i are set according to equation (15) (see Table 4). The filter was executed offline, and the biases and noises were obtained from the IMU's datasheet. Figure 1 shows the measurements of the angular velocities vector (i.e., the input vector) $u = \omega^T = [p \ q \ r]^T$ (see transition model (19)), the linear accelerations vector $a = \begin{bmatrix} a_x & a_y & a_z \end{bmatrix}^T$ and the earth's magnetic vector $h = \begin{bmatrix} h_x & h_y & h_z \end{bmatrix}^T$ (see measurement model (22)).

a)

b)

c)
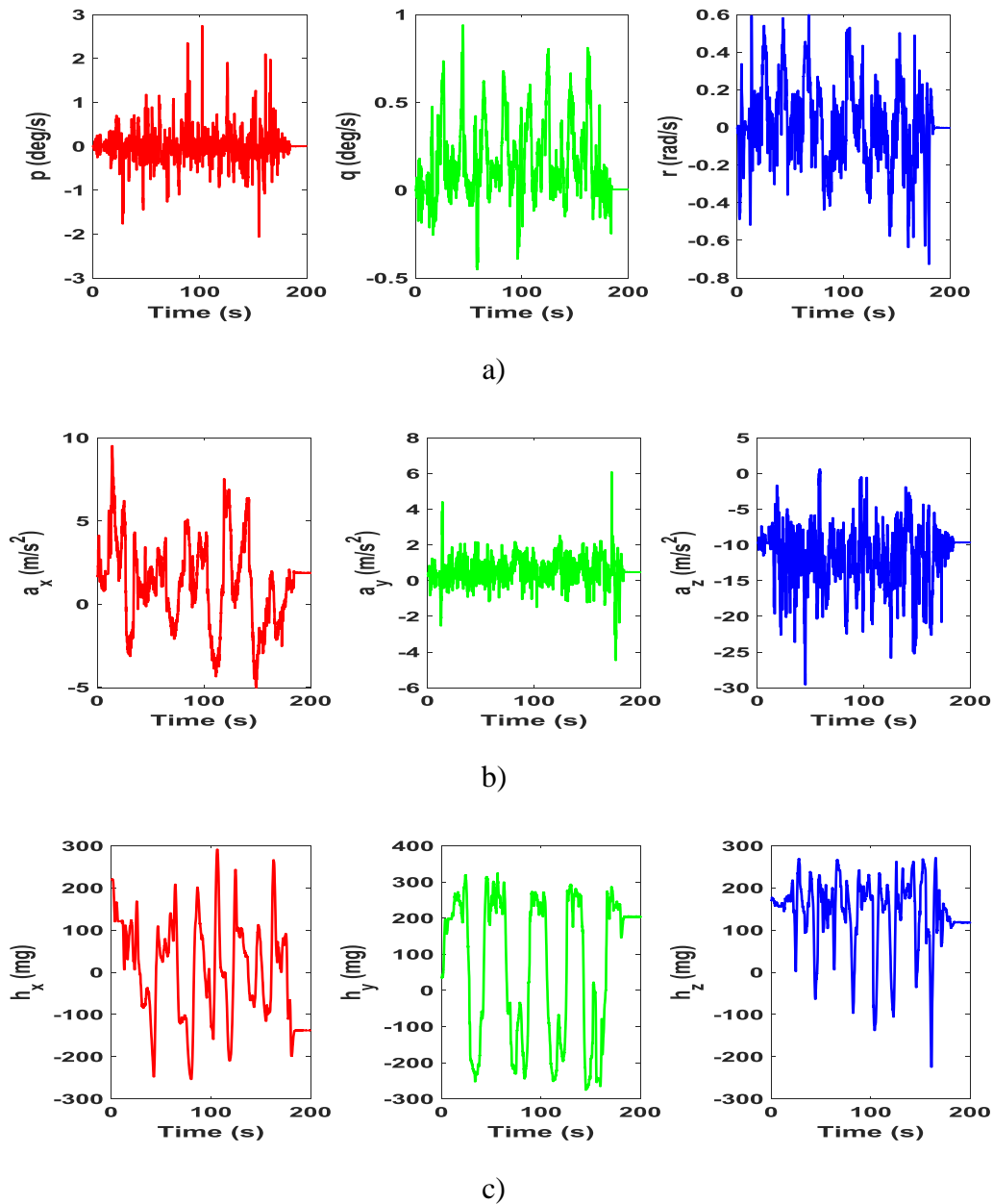
Figure 1. Measurements provided by the UAV's IMU and magnetometer instruments:

a)gyroscope measurements, b) accelerometer measurements, c) magnetometer measurements.

Figures 2. and 3 show the estimates of the UAV attitude and the biases of the gyroscope. From these results it can be seen how the performance of the proposed algorithm is accurate and the convergence is smoother. Moreover, the estimator is stable over the flight period.
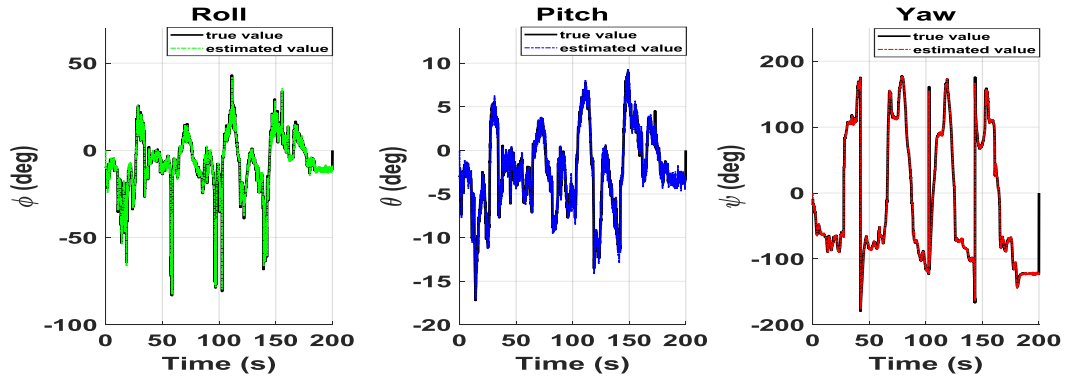
Figure 2. UAV attitude estimation using AE-UKF a) roll angle, b) pitch angle, c) yaw angle.
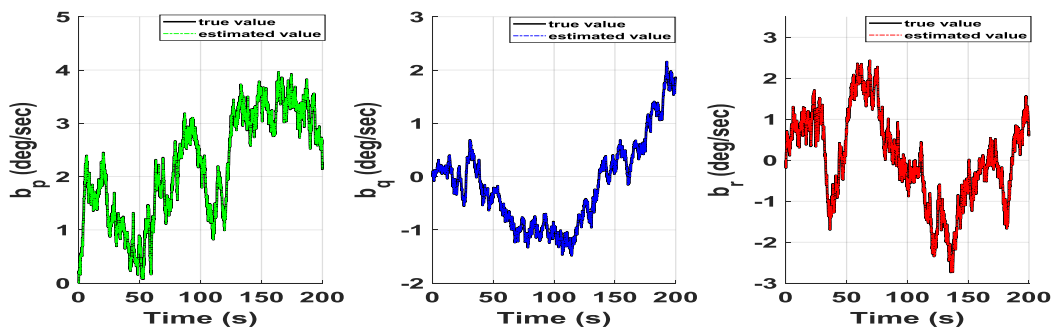
Figure 3. Gyro biases estimation using AE-UKF a) roll axis, b) pitch axis, c) yaw axis.

To achieve an ensemble average of estimating errors, we compute the estimation-error covariance $\mathbf{\Gamma}$, lower and upper limits of deviations $\sigma_{min} = \min(\mathbf{\Gamma})$ and $\sigma_{max}\max(\mathbf{\Gamma})$, and RMSE (root-mean squared error) s as follows

$$\begin{cases} \boldsymbol{\xi}_i = \boldsymbol{x}_{i,m} - \widetilde{\boldsymbol{x}}_i \\ \mathbf{\Gamma} = \frac{1}{N}\sum_{i=1}^{N} \boldsymbol{\xi}_i \boldsymbol{\xi}_i^T \\ s = \sqrt{\frac{1}{N}\sum_{i=1}^{N} \mathbf{\Gamma}_i} \end{cases} \tag{30}$$

where N denotes the length of the data set, and $\widetilde{\boldsymbol{x}}_i$, $\boldsymbol{x}_{i,m}, \boldsymbol{\xi}_i$ denote the state estimate, state measurement, and error vectors at each time step. Table 4 summarizes the analysis results for different standard deviations μ_i.

Table 4. Standard deviations of estimation-error covariance and RMSEs

Instrument	$\mu_i = 0.1$	$\mu_i = 1$	$\mu_i = 10$
σ_{min}	7.0626e-9	1.9468e-10	4.4869e-9
σ_{max}	0.0192	0.0185	0.0154
s	0.0059	0.0073	0.0200

| $\bar{s} = s/(\sigma_{max} - \sigma_{min})$ | 0.3067 | 0.3957 | 1.3012 |

From the results shown in Table 4, we find that the gradient $\Delta \tilde{P}_{i,k}$ shown in equation (12) is sensitive to the eigenvalues μ_i and its limit (15) depends on the choice of the matrix R. Although the proposed process noise model aided in the investigation of the sensitivity of the estimation-error covariance, theoretical extension to include new process and measurement noise models is possible.

5.   Conclusion

In this paper, a novel EKF for attitude estimation of a lightweight UAV was designed. Due to the UAV's nonlinear kinematics and dynamics, nonlinear Kalman filtering is a typical solution for attitude estimation. An EKF algorithm for determining the three-attitude orientation as well as the gyros biases has been developed and its sensitivity was investigated. The algorithm's performance has been validated via simulation and evaluated by field test data gathered onboard of an UltraStick e25 UAV. The method is extremely suitable for future implementation on an onboard system with limited electronic resources. The results enable assurance to pursue guidance, navigation, and control tasks in real time.

Acknowledgement

Reference

[1] Y Crain., R.H., Bishop, & T. Brady, Shifting the Inertial Navigation Paradigm with MEMS Technology. *Advanced in the Astronautical Sciences,* 137, 2010.

[2] Anam Tahir, Jari Böling, Mohammad-Hashem Haghbayan, Hannu T. Toivonen, Juha Plosila, Swarms of Unmanned Aerial Vehicles — A Survey, Journal of Industrial Information Integration, Volume 16, 2019.

[3] A. Lamba, G. Tamrakar, H. Gaur, Simulation of a UAV-based wireless sensor network on NS-3 to analyze IEEE 802.11 performance, Mathematical Statistician and Engineering Applications, 71(4), 2022, 6722-6737.

[4] F.L., Markley, Attitude error representations for Kalman filtering. *Journal of Guidance, Control, and Dynamics*, *63*(2), 2003, 311-317.

[5] S.C., Stubberud, & K.A., Kramer, Predictive guidance intercept using the neural extended Kalman filter tracker, *Mechatronic systems and control (formerly control and intelligent systems)*, *35*(3), 2007, 228-235.

[6] R.T. Bambang, K. Uchida, & R.R. Yacoub, Active noise control in free space using recurrent neural networks with EKF algorithm, *Mechatronic systems and control (formerly control and intelligent systems)*, *36*(3), 2008, 267-276.

[7] S. Bonnabel, P. Martin P., & E. Salaun. Invariant extended Kalman filter: theory and application to a velocity-aided attitude estimation problem. *Proceedings of the 48th IEEE Conference on Decision and Control*, 2009, 1297-1304

[8] X., Jing, J., Cui1, H., He, B., Zhang, D., Ding, & Y., Yang, Attitude estimation for UAV using extended Kalman filter, 29th Chinese Control and Decision Conference (CCDC), 2017, 3307-3312.

[9] F.L., Markley, J.L., Crassidis, & Y., Cheng. Nonlinear Attitude Filtering Methods. *In Proceedings of AIAA Guidance, Navigation and Control Conference*, San Francisco, CA, USA, 2005, 1-32.

[10] B.O.S.,Teixeira, L.A.B., Tôrres, P., Iscold, & L.A., Aguirre, Flight path reconstruction – a comparison of nonlinear Kalman filter and smoother algorithms, *Aerospace Science and Technology*, *15*, 2011, 60-71.

[11] J.J., Xiong, & E.H., Zheng, Optimal Kalman filter for state estimation of a quadrotor UAV. *Optik*, *126*, 2015, 2862-2868.

[12] B.A., Li, Z.H., Liu, & S.F., Li, Research of UAV fault and state forecast technology based on particle filter. *Proceeding of IEEE Autotestcon*, Beijing, China, 2009, 14−17.

[13] L., Xiang, C., He, Y., Wang, & Z., Li, Generalized complementary filter for attitude estimation based on vector observations and cross products. *Proceeding of the IEEE International Conference on Information and Automation*, China, 2015, 1733-1737.

[14] Y. Zhang, J. Wu, C. Yang and X. Zhang, "Complementary filter based on quaternion for outdoor navigation of UAV," 2018 IEEE CSAA Guidance, Navigation and Control Conference (CGNCC), Xiamen, China, 2018, pp. 1-6, doi: 10.1109/GNCC42960.2018.9019141.

[15] Bassolillo, S.R.; D'Amato, E.; Notaro, I.; Ariante, G.; Del Core, G.; Mattei, M. Enhanced Attitude and Altitude Estimation for Indoor Autonomous UAVs. Drones 2022, 6, 18.

[16] Liu, N.; Qi, W.; Su, Z.; Feng, Q.; Yuan, C. Research on Gradient-Descent Extended Kalman Attitude Estimation Method for Low-Cost MARG. Micromachines 2022, 13, 1283.

[17] H.G., De-Marina, F.J., Pereda, & J.M., Giron-Sierra, Adaptive UAV Attitude Estimation Employing Unscented Kalman Filter, FOAM and Low-cost MEMS Sensors. *Sensors*, *12*, 2012, 9566-9585.

[18] M., Zamani, J., Trumpf, & R., Mahony, Minimum-Energy Filtering for Attitude Estimation, *American Control Conference,* Portland, OR, 2013, 4943-4948.

[19] M., Zamani, J., Trumpf, & R., Mahony, On the distance to optimality of the geometric approximate minimum-energy attitude filter. *IEEE transactions on Automatic Control, 58*(11), 2014, 2917-2921.

[20] M., Zamani, J., Trumpf, & R., Mahony, Nonlinear attitude filtering: a comparison study, *rXiv preprint arXiv*:1502.03990, *11*, 2015.

[21] E., Fresk, & G., Nikolakopoulos, Full quaternion-based attitude control for a quadrotor. *European Control Conference (ECC)*, Zürich, Switzerland, 2013, 3864-3869.